

# Measurement of the half-life of the two-neutrino double beta decay of $^{76}\text{Ge}$ with the GERDA experiment

The GERDA Collaboration

M Agostini<sup>14</sup>, M Allardt<sup>3</sup>, E Andreotti<sup>5,18</sup>,  
 A M Bakalyarov<sup>12</sup>, M Balata<sup>1</sup>, I Barabanov<sup>10</sup>,  
 M Barnabé Heider<sup>14‡</sup>, N Barros<sup>3</sup>, L Baudis<sup>19</sup>, C Bauer<sup>6</sup>,  
 N Becerici-Schmidt<sup>13</sup>, E Bellotti<sup>7,8</sup>, S Belogurov<sup>11,10</sup>,  
 S T Belyaev<sup>12</sup>, G Benato<sup>19</sup>, A Bettini<sup>15,16</sup>, L Bezrukov<sup>10</sup>,  
 T Bode<sup>14</sup>, V Brudanin<sup>4</sup>, R Brugnera<sup>15,16</sup>, D Budjáš<sup>14</sup>,  
 A Caldwell<sup>13</sup>, C Cattadori<sup>8</sup>, A Chernogorov<sup>11</sup>,  
 F Cossavella<sup>13</sup>, E V Demidova<sup>11</sup>, A Denisov<sup>10</sup>, A Domula<sup>3</sup>,  
 V Egorov<sup>4</sup>, R Falkenstein<sup>18</sup>, A D Ferella<sup>19</sup>, K Freund<sup>18</sup>,  
 F Froborg<sup>19</sup>, N Frodyma<sup>2</sup>, A Gangapshev<sup>10,6</sup>,  
 A Garfagnini<sup>15,16</sup>, S Gazzana<sup>6</sup>, P Grabmayr<sup>18</sup>,  
 V Gurentsov<sup>10</sup>, K Gusev<sup>4,12,14</sup>, K K Guthikonda<sup>19</sup>,  
 W Hampel<sup>6</sup>, A Hegai<sup>18</sup>, M Heisel<sup>6</sup>, S Hemmer<sup>15,16</sup>,  
 G Heusser<sup>6</sup>, W Hofmann<sup>6</sup>, M Hult<sup>5</sup>, L V Inzhechik<sup>10§</sup>,  
 L Ioannucci<sup>1</sup>, J Janicskó Csáthy<sup>14</sup>, J Jochum<sup>18</sup>, M Junker<sup>1</sup>,  
 S Kianovsky<sup>10</sup>, I V Kirpichnikov<sup>11</sup>, A Kirsch<sup>6</sup>,  
 A Klimenko<sup>4,10,6</sup>, K T Knöpfle<sup>6</sup>, O Kochetov<sup>4</sup>,  
 V N Kornoukhov<sup>11,10</sup>, V Kusminov<sup>10</sup>, M Laubenstein<sup>1</sup>,  
 A Lazzaro<sup>14</sup>, V I Lebedev<sup>12</sup>, B Lehnert<sup>3</sup>, H Y Liao<sup>13</sup>,  
 M Lindner<sup>6</sup>, I Lippi<sup>16</sup>, X Liu<sup>17</sup>, A Lubashevskiy<sup>6</sup>,  
 B Lubsandorzhiev<sup>10</sup>, G Lutter<sup>5</sup>, A A Machado<sup>6</sup>,  
 B Majorovits<sup>13</sup>, W Maneschg<sup>6</sup>, I Nemchenok<sup>4</sup>, S Nisi<sup>1</sup>,  
 C O'Shaughnessy<sup>13</sup>, L Pandola<sup>1||</sup>, K Pelczar<sup>2</sup>, L Peraro<sup>15,16</sup>,  
 A Pullia<sup>9</sup>, S Riboldi<sup>9</sup>, F Ritter<sup>18¶</sup>, C Sada<sup>15,16</sup>, M Salathe<sup>6</sup>,  
 C Schmitt<sup>18</sup>, S Schönert<sup>14</sup>, J Schreiner<sup>6</sup>, O Schulz<sup>13</sup>,  
 B Schwingenheuer<sup>6</sup>, E Shevchik<sup>4</sup>, M Shirchenko<sup>12,4</sup>,  
 H Simgen<sup>6</sup>, A Smolnikov<sup>6</sup>, L Stanco<sup>16</sup>, H Strecker<sup>6</sup>,  
 M Tarka<sup>19</sup>, C A Ur<sup>16</sup>, A A Vasenko<sup>11</sup>, O Volynets<sup>13</sup>,  
 K von Sturm<sup>18</sup>, M Walter<sup>19</sup>, A Wegmann<sup>6</sup>, M Wojcik<sup>2</sup>,  
 E Yanovich<sup>10</sup>, P Zavarise<sup>1+</sup>, I Zhitnikov<sup>4</sup>, S V Zhukov<sup>12</sup>,  
 D Zinatulina<sup>4</sup>, K Zuber<sup>3</sup> and G Zuzel<sup>2</sup>

<sup>1</sup> INFN Laboratori Nazionali del Gran Sasso, LNGS, Assergi, Italy

<sup>2</sup> Institute of Physics, Jagiellonian University, Cracow, Poland

‡ *Present Address:* CEGEP St-Hyacinthe, Québec, Canada

§ *Present Address:* Moscow Institute of Physics and Technology, Russia

|| *Present Address:* Corresponding Author

¶ *Present Address:* Robert Bosch GmbH, Reutlingen, Germany

+ *Present Address:* University of L'Aquila, Dipartimento di Fisica, L'Aquila, Italy

- <sup>3</sup> Institut für Kern- und Teilchenphysik, Technische Universität Dresden, Dresden, Germany  
<sup>4</sup> Joint Institute for Nuclear Research, Dubna, Russia  
<sup>5</sup> Institute for Reference Materials and Measurements, Geel, Belgium  
<sup>6</sup> Max-Planck-Institut für Kernphysik, Heidelberg, Germany  
<sup>7</sup> Dipartimento di Fisica, Università Milano Bicocca, Milano, Italy  
<sup>8</sup> INFN Milano Bicocca, Milano, Italy  
<sup>9</sup> Dipartimento di Fisica, Università degli Studi di Milano e INFN Milano, Milano, Italy  
<sup>10</sup> Institute for Nuclear Research of the Russian Academy of Sciences, Moscow, Russia  
<sup>11</sup> Institute for Theoretical and Experimental Physics, Moscow, Russia  
<sup>12</sup> National Research Centre “Kurchatov Institute”, Moscow, Russia  
<sup>13</sup> Max-Planck-Institut für Physik, München, Germany  
<sup>14</sup> Physik Department and Excellence Cluster Universe, Technische Universität München, Germany  
<sup>15</sup> Dipartimento di Fisica e Astronomia dell’Università di Padova, Padova, Italy  
<sup>16</sup> INFN Padova, Padova, Italy  
<sup>17</sup> Shanghai Jiaotong University, Shanghai, China  
<sup>18</sup> Physikalisches Institut, Eberhard Karls Universität Tübingen, Tübingen, Germany  
<sup>19</sup> Physik Institut der Universität Zürich, Zürich, Switzerland
- E-mail: [pandola@lngs.infn.it](mailto:pandola@lngs.infn.it)

**Abstract.** The primary goal of the GERmanium Detector Array (GERDA) experiment at the Laboratori Nazionali del Gran Sasso of INFN is the search for the neutrinoless double beta decay of  $^{76}\text{Ge}$ . High-purity germanium detectors made from material enriched in  $^{76}\text{Ge}$  are operated directly immersed in liquid argon, allowing for a substantial reduction of the background with respect to predecessor experiments. The first 5.04 kg-yr of data collected in Phase I of the experiment have been analyzed to measure the half-life of the neutrino-accompanied double beta decay of  $^{76}\text{Ge}$ . The observed spectrum in the energy range between 600 and 1800 keV is dominated by the double beta decay of  $^{76}\text{Ge}$ . The half-life extracted from GERDA data is  $T_{1/2}^{2\nu} = (1.84_{-0.10}^{+0.14}) \cdot 10^{21}$  yr.

PACS numbers: 23.40.-s, 07.85.Fv

Submitted to: *J. Phys. G: Nucl. Part. Phys.*

## 1. Introduction and scope

Neutrinoless double beta ( $0\nu\beta\beta$ ) decay of atomic nuclei  $(A,Z) \rightarrow (A,Z+2) + 2e^-$  is a forbidden process in the Standard Model (SM) of particle physics because it violates lepton number by two units. An observation of such a decay would demonstrate lepton number violation in nature and would prove that neutrinos have a Majorana component. For recent reviews, see [1]. The two-neutrino double beta ( $2\nu\beta\beta$ ) decay of atomic nuclei,

$$(A, Z) \rightarrow (A, Z + 2) + 2e^- + 2\bar{\nu}_e,$$

with the simultaneous emission of two electrons and two anti-neutrinos, conserves lepton number and is allowed within the SM, independent of the nature of the neutrino. Being a higher-order process, it is characterized by an extremely low decay rate: so far it is the rarest decay observed in laboratory experiments. It is observable for a few even-even nuclei and was detected to-date for eleven nuclides; the corresponding half-lives are in the range of  $7 \cdot 10^{18} - 2 \cdot 10^{24}$  yr [2, 3, 4].

The measurement of the half-life of the  $2\nu\beta\beta$  decay ( $T_{1/2}^{2\nu}$ ) is of substantial interest. For example, model predictions of the  $0\nu\beta\beta$  half-life require the evaluation of nuclear matrix elements. These calculations are complicated and have large uncertainties. They are different from those required for the  $2\nu\beta\beta$  decay, but it has been suggested [5, 6] that, within the same model framework, some constraints on the  $0\nu\beta\beta$  matrix elements  $\text{NME}^{0\nu}$  can be derived from the knowledge of the  $2\nu\beta\beta$  nuclear matrix elements  $\text{NME}^{2\nu}$ . Also, the nuclear matrix element  $\text{NME}^{2\nu}$  which is extracted from the measurement of the half-life of the  $2\nu\beta\beta$  decay can be directly compared with the predictions based on charge exchange experiments [7, 8]. A good agreement would indicate that the reaction mechanisms and the nuclear structure aspects that are involved in the  $2\nu\beta\beta$  decay are well understood.

The GERmanium Detector Array (GERDA) experiment at the Laboratori Nazionali del Gran Sasso of INFN searches for the  $0\nu\beta\beta$  decay of  $^{76}\text{Ge}$ . High-purity germanium detectors isotopically enriched in  $^{76}\text{Ge}$  are operated bare and immersed in liquid argon in order to greatly reduce the environmental background. As a first result of this ongoing research, the present paper reports a precise measurement of the half-life of the  $2\nu\beta\beta$  decay of  $^{76}\text{Ge}$ . The data used in this work encompasses an exposure of 5.04 kg·yr, taken between November 2011 and March 2012.

## 2. The GERDA experimental setup

A brief outline of the components of the GERDA detector that are most relevant for this work is given below; a detailed description can be found in [9, 10].

The GERDA experimental setup is shown in figure 1. At the core of the setup there is an array of high-purity germanium detectors (HPGe). They are operated bare in liquid argon (LAr) which acts both as a coolant and as a shield against the residual environmental background. The array configuration consists of eleven germanium detectors: eight are made from isotopically modified germanium ( $^{\text{enr}}\text{Ge}$ ), enriched to about 86% in  $^{76}\text{Ge}$ , and three are made from natural germanium ( $^{\text{nat}}\text{Ge}$ ), with a total



**Figure 1.** Artist's view of the GERDA experiment. The detector array is not to scale.

mass of 17.67 kg and 7.59 kg, respectively. The enriched detectors come from the former Heidelberg-Moscow (HDM) [11] and IGEX [12] experiments. They underwent specific refurbishing processes before operation in GERDA [13, 14]. The germanium detectors are mounted in strings with typically three diodes each. Signals are amplified by low noise, low radioactivity charge sensitive preamplifiers [15] with 30 MHz bandwidth operated inside the LAr. They are digitized by a 14-bit 100 MHz continuously running ADC (FADC) equipped with anti-aliasing bandwidth filters. In the offline analysis the waveforms are digitally processed to reconstruct the event energy.

The detector array is surrounded by  $64\text{ m}^3$  of 5.0-grade LAr, contained in a vacuum insulated cryostat made of stainless steel, lined on the inner side by a 3 to 6 cm thick layer of copper. The cryostat is in turn placed at the centre of a  $580\text{ m}^3$  volume of ultra-pure water equipped with 66 photomultiplier tubes to veto the residual cosmic ray muons by the detection of Cherenkov light. The large water volume also serves as a shield to moderate and capture neutrons produced by natural radioactivity and in muon-induced hadronic showers.

The energy scale is set by using calibration curves, parametrized as second-order polynomials, derived for each detector by calibration runs taken with  $^{228}\text{Th}$  sources. The stability of the energy scale is monitored by performing such calibration runs every one or two weeks. Moreover, the stability of the system is continuously monitored by using ad hoc charge pulses generated by a spectroscopy pulser that are regularly injected in the input of the charge sensitive preamplifier.

All GERDA detectors but two exhibit a reverse current of the order of tens of pA. The two problematic detectors showed an increase of leakage current soon after the beginning of their operation; therefore their bias high voltage had to be reduced and finally completely removed. These two detectors do not contribute to the present

data set, although they are accounted for in the detector anti-coincidence cut described below. The total mass of the operational enriched detectors is 14.63 kg. The  $^{\text{nat}}\text{Ge}$  detectors are not considered in the present analysis because of their low content of  $^{76}\text{Ge}$ . The average energy resolution for the six enriched detectors considered in this study is about 4.5 keV (full width at half maximum) at the  $Q_{\beta\beta}$ -value of  $^{76}\text{Ge}$  (2039 keV) [10].

A key parameter which is required for the computation of  $T_{1/2}^{2\nu}$  is the total  $^{76}\text{Ge}$  active mass. It is calculated as the product of the total detector mass with the isotopic abundance of  $^{76}\text{Ge}$  ( $f_{76}$ ) and the fraction of the active mass ( $f_{act}$ ).

The average  $^{76}\text{Ge}$  isotopic abundance of the six enriched detectors considered in this work is 86.3% [10, 12, 16, 17].

In GERDA p-type semi-coaxial detectors are used, for which a part of the volume close to the outer surface is inactive. After mechanical modifications and processing of the germanium diodes at the manufacturer, their active mass was re-determined experimentally [10, 13]. The measured average fraction  $f_{act}$  is 86.7%, with individual detector  $f_{act}$  uncertainties of about 6.5%.

### 3. The data set

The data set considered for the analysis was taken between November 9, 2011, and March 21, 2012, for a total of 125.9 live days, amounting to an exposure of 5.04 kg·yr. Digitized charge pulses from the detectors are analyzed with the software tool GELATIO [18] according to the GERDA standard procedure [19]. The pulse amplitude is reconstructed offline by applying an approximated Gaussian filter with an integration time of 5  $\mu\text{s}$  (which is sufficient to avoid losses due to ballistic effects). Events generated by discharges or due to electromagnetic noise are rejected by using a set of quality cuts. Due to the low counting rate, the data set has a negligible contamination of pile-up events. The combined efficiency of the trigger and of the offline data processing is practically 100% above 100 keV. Similarly, no loss of physical events is expected from the application of the quality cuts, as deduced by dedicated Monte Carlo studies and by the analysis of pulser data. Events that are in coincidence with a valid veto signal from the muon detector and events having a signal in more than one HPGe detector are excluded from the analysis. The time window for the coincidence between the muon detector and the HPGe detectors was set to 8  $\mu\text{s}$  while that between different HPGe detectors was set to a few  $\mu\text{s}$ . Due to the very low muon flux in the Gran Sasso laboratory, the dead time induced by the muon veto is negligible.

Given the half-life of the  $2\nu\beta\beta$  decay reported in the literature (about  $1.5 \cdot 10^{21}$  yr), the anticipated count rate of the  $^{\text{enr}}\text{Ge}$  detectors is about 100 counts/day in the entire energy range up to  $Q_{\beta\beta}=2039$  keV. Since the detectors are submerged in LAr, the radioactive decay of  $^{39}\text{Ar}$ , which is a long-lived  $\beta$  emitter produced by cosmogenic activation of natural argon in the atmosphere, gives a large contribution up to its  $Q_{\beta}$ -value of 565 keV. In fact, the low-energy spectrum is dominated by these  $\beta$  particles and their Bremsstrahlung photons, which account for about 1000 counts/day above 100 keV. The  $2\nu\beta\beta$  decay is expected to be the major contributor in the energy spectrum above the end-point of the  $^{39}\text{Ar}$  spectrum. For this reason, the analysis of the  $2\nu\beta\beta$  decay is performed in the range between 600 keV, which is comfortably above the end-point of the  $^{39}\text{Ar}$  spectrum, and 1800 keV. The sum spectrum of the

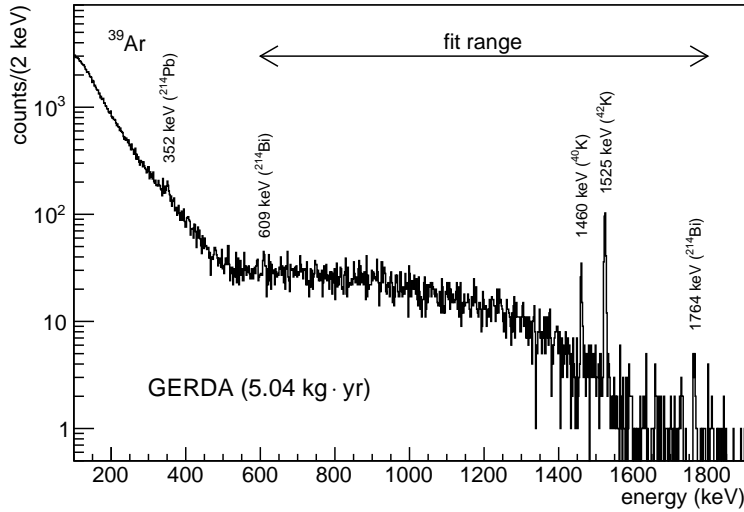


**Figure 2.** Energy spectrum of the six  $^{\text{enr}}\text{Ge}$  detectors. The  $^{39}\text{Ar}$   $\beta$  decay dominates the counting rate at low energies up to its  $Q_{\beta}$ -value of 565 keV. The energy range which is considered for the  $2\nu\beta\beta$  analysis and a few prominent  $\gamma$  lines are also shown.

six  $^{\text{enr}}\text{Ge}$  detectors considered in this work is displayed in figure 2. The analysis range contains 8796 events in total. The probability for a  $2\nu\beta\beta$  decay taking place in the active volume of the  $^{\text{enr}}\text{Ge}$  detectors to produce a total energy release between 600 and 1800 keV is about 63.5%; the energy range above 1800 keV is practically insensitive to the  $2\nu\beta\beta$  signal, as the probability for a decay to produce an energy release in this region is  $< 0.02\%$ . These estimates are based on the Monte Carlo simulation of  $2\nu\beta\beta$  decays in the GERDA detectors as described in section 4. Hence, the energy region chosen for the analysis is well suited for the study of the  $2\nu\beta\beta$  decay signal.

## 4. Data analysis

### 4.1. Statistical treatment and fit model

The experimental spectra of the six diodes are analyzed following the binned maximum likelihood approach described in [20]. The analysis region is divided into 40 bins, each 30 keV wide. A global model is fitted to the observed energy spectra. The model contains the  $2\nu\beta\beta$  decay of  $^{76}\text{Ge}$  and three independent background contributions, namely  $^{42}\text{K}$ ,  $^{214}\text{Bi}$  and  $^{40}\text{K}$ . The presence of these background sources is established by the observation of their characteristic  $\gamma$  lines: 1525 keV from  $^{42}\text{K}$ ; 1460 keV from  $^{40}\text{K}$ ; 609 keV and 1764 keV from  $^{214}\text{Bi}$ ; 352 keV from  $^{214}\text{Pb}$  (progenitor of  $^{214}\text{Bi}$ ).

$^{42}\text{K}$  is a short-lived  $\beta$  emitter ( $Q_{\beta} = 3525$  keV,  $T_{1/2} = 12.6$  h) which is present in GERDA as a progeny of the long-lived  $^{42}\text{Ar}$  ( $Q_{\beta} = 599$  keV,  $T_{1/2} = 32.9$  yr).  $^{42}\text{Ar}$  is a trace radioactive contaminant expected in natural argon and is produced by cosmogenic activation.  $^{214}\text{Bi}$  from the  $^{238}\text{U}$  decay series and  $^{40}\text{K}$  are  $\gamma$  emitters from the

environmental radioactivity.

A few more candidate  $\gamma$  lines have been identified in the GERDA spectrum [10], which indicate the presence of small additional background contributions: in particular  $^{208}\text{Tl}$  and  $^{228}\text{Ac}$  from the  $^{232}\text{Th}$  decay series, and  $^{60}\text{Co}$ . However, most of the candidate  $\gamma$  lines have either a poor statistical significance and/or are seen in some detectors only. Given the lack of discriminating power in the data, the background contributions other than  $^{42}\text{K}$ ,  $^{214}\text{Bi}$  and  $^{40}\text{K}$  are not included in the fit. However, their possible impact on the extracted half-life  $T_{1/2}^{2\nu}$  is included in the systematic uncertainty, as discussed in section 4.2; their cumulative contribution to the background is estimated to be of a few percent.

The half-life of the  $2\nu\beta\beta$  decay is common in the fit to the six spectra of the  $^{\text{enr}}\text{Ge}$  detectors. The intensities of the background components are independent for each detector. The active mass and the  $^{76}\text{Ge}$  abundance of each detector are also left free in the fit; they are treated as nuisance parameters and integrated over at the end of the analysis.

The shapes of the energy spectra for the model components (signal and three backgrounds) are derived by a Monte Carlo simulation for each detector individually. The simulation is performed using the MAGE framework [21] based on GEANT4 [22]. Assumptions have to be made in the Monte Carlo simulation about the location and the primary spectrum of each component of the model. The spectrum of the two electrons emitted in the  $2\nu\beta\beta$  decay of  $^{76}\text{Ge}$  is sampled according to the distribution of [3] that is implemented in the code DECAY0 [23]. Electrons are propagated in the GERDA simulated setup by MAGE and the total energy released in the active mass of the enriched detectors is registered.

The  $^{42}\text{K}$  activity is uniformly distributed in the liquid argon volume. The decay products of the  $\beta$  decay of  $^{42}\text{K}$  are taken into account as the initial state in the simulation. However the energy deposit in the detectors is mainly given by the 1525 keV  $\gamma$ -ray (full energy peak and Compton continuum): the contribution due to the  $\beta$  particles is small (less than a few percent) with respect to the 1525 keV  $\gamma$ -ray. The actual position of the  $^{40}\text{K}$  and  $^{214}\text{Bi}$  emitters contributing to the GERDA spectrum is not known in detail: the assumption is made in the Monte Carlo of “close sources”. The ratio of the intensities of the  $^{214}\text{Bi}$   $\gamma$  lines observed in the experimental spectrum is consistent with such an assumption. The impact on  $T_{1/2}^{2\nu}$  due to the lack of knowledge about the source position – which affects the peak-to-Compton ratio – is accounted as a systematic uncertainty. The effect of muon-induced events that are not accompanied by a veto signal, e.g. due to inefficiency, is estimated to be  $< 0.02\%$  in the energy range of this analysis.

The spectral fit is performed using the Bayesian Analysis Toolkit BAT [24]. A flat distribution between 0 and  $10^{22}$  yr is taken as the prior probability density function (pdf) for  $T_{1/2}^{2\nu}$ . The prior pdf for the active mass fraction of each detector is modelled as a Gaussian distribution, having mean value and standard deviation according to the measurements performed in [13]. The analysis accounts for the fact that the uncertainties on the active masses  $f_{act}$  are partially correlated, because of the experimental procedure employed for the measurement. Uncertainties on  $f_{act}$  are split into an uncorrelated term – which is specific of each detector – and a common correlated term. The prior pdf for the  $^{76}\text{Ge}$  isotopic abundance  $f_{76}$  for each detector is also a

detector	total mass (g)	active mass (g)	$^{76}\text{Ge}$ isotopic abundance (%)	$T_{1/2}^{2\nu}$ ( $10^{21}$ yr)
ANG2	2833	2468±121±89	86.6±2.5	1.99 $^{+0.14}_{-0.15}$
ANG3	2391	2070±118±77	88.3±2.6	1.69 $^{+0.15}_{-0.14}$
ANG4	2372	2136±116±79	86.3±1.3	1.94 $^{+0.14}_{-0.15}$
ANG5	2746	2281±109±82	85.6±1.3	1.79 $^{+0.12}_{-0.14}$
RG1	2110	1908±109±72	85.5±2.0	1.94 $^{+0.18}_{-0.14}$
RG2	2166	1800±99±65	85.5±2.0	1.93 $^{+0.16}_{-0.16}$

**Table 1.** Summary table of the six enriched detectors used in this work. For each detector, the total mass, the active mass and the isotopic abundance of  $^{76}\text{Ge}$  are given. The uncertainties reported for the active masses are the uncorrelated (first) and correlated (second) errors. The last column reports the  $T_{1/2}^{2\nu}$  which is obtained by performing the analysis on each detector individually. The uncertainty on  $T_{1/2}^{2\nu}$  is the fit uncertainty only.

Gaussian, having mean value according to the earlier measurements reported in [10]. The uncertainty of  $f_{76}$  is between 1% and 3% for the single detectors. It was estimated from the dispersion of independent measurements performed with isotopically enriched material; this dispersion is much larger than the quoted uncertainty of each individual measurement.

The fit has 32 free parameters: one common value for the  $2\nu\beta\beta$  half-life and 31 nuisance parameters. The nuisance parameters are the common term which describes the correlated uncertainty of the active masses plus five independent variables for each of the six detectors (active mass,  $^{76}\text{Ge}$  abundance and three background components). The detector parameters used for the prior pdf's are summarized in table 1.

Figure 3 shows experimental data together with the best fit model for the sum of the six detectors. The analysis energy window contains 8796 events. The best fit model has an expectation of 8797.0 events, divided as follows: 7030.1 (79.9%) from the  $2\nu\beta\beta$  decay of  $^{76}\text{Ge}$ ; 1244.6 (14.1%) from  $^{42}\text{K}$ ; 335.5 (3.8%) from  $^{214}\text{Bi}$ ; and 186.8 (2.1%) from  $^{40}\text{K}$ . The individual components derived from the fit are also shown in figure 3. The signal-to-background ratio in the region 600–1800 keV is on average 4 : 1, which is much better than for any past experiment which observed the  $2\nu\beta\beta$  decay of  $^{76}\text{Ge}$ . The best ratio achieved so far for  $^{76}\text{Ge}$  was approximately 1 : 1 by HDM [17]. The model is able to reproduce well the experimental data, as shown in the lower panel of figure 3. The  $p$ -value of the fit derived from the procedure of [25], is  $p = 0.77$ . All nuisance parameters are eventually integrated over in order to derive the posterior pdf  $p(T_{1/2}^{2\nu})$  for the  $2\nu\beta\beta$  half-life. The  $p(T_{1/2}^{2\nu})$  distribution is nearly Gaussian; the best estimate of the half-life is

$$T_{1/2}^{2\nu} = (1.84^{+0.09}_{-0.08}) \cdot 10^{21} \text{ yr}, \quad (1)$$

(fit error only). This uncertainty is calculated as the smallest interval containing 68% probability of  $p(T_{1/2}^{2\nu})$ . It includes the uncertainty induced on  $T_{1/2}^{2\nu}$  by the nuisance parameters of the fit and accounts for parameter correlations. Active masses and  $^{76}\text{Ge}$  isotopic abundances drive the fit uncertainty on  $T_{1/2}^{2\nu}$ : if these parameters were known without uncertainties, the  $1\sigma$  uncertainty from the fit would be about  $0.03 \cdot 10^{21}$  yr.

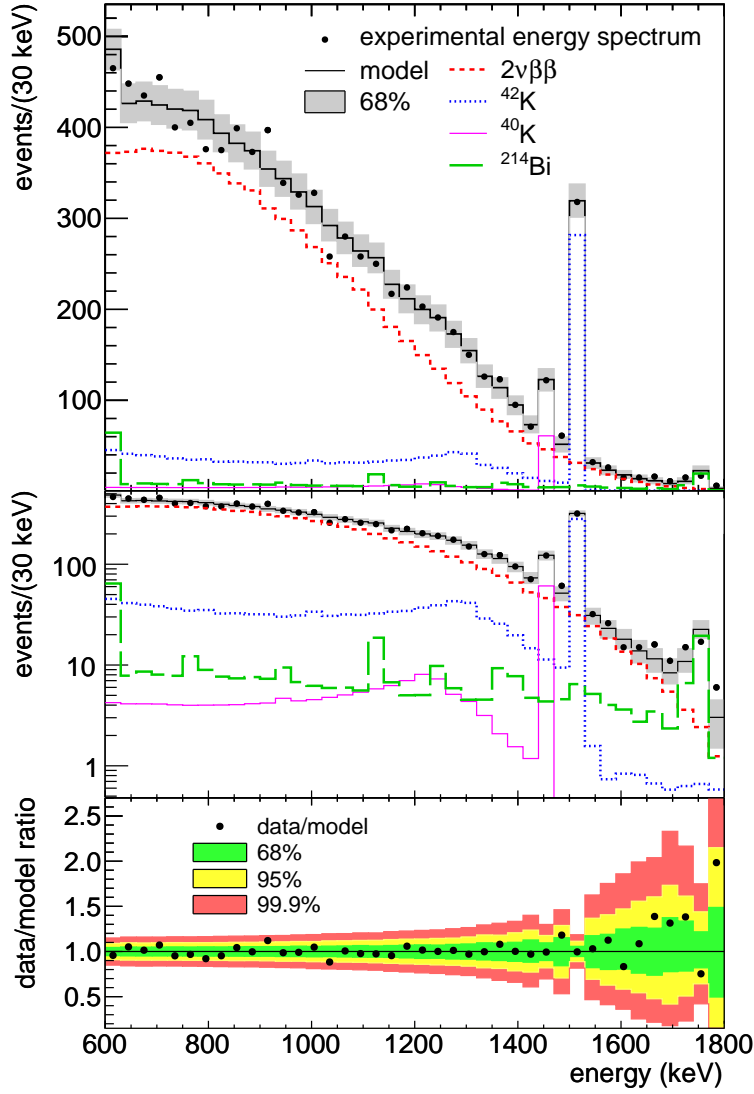


**Figure 3.** Upper and middle panels: Experimental data (markers) and the best fit model (black histogram) for the sum of the six detectors together (linear and logarithmic scale). Individual contributions from  $2\nu\beta\beta$  decay (red),  $^{42}\text{K}$  (blue),  $^{40}\text{K}$  (purple) and  $^{214}\text{Bi}$  (green) are shown separately. The shaded band covers the 68% probability range for the data calculated from the expected event counts of the best fit model. Lower panel: ratio between experimental data and the prediction of the best fit model. The green, yellow and red regions are the smallest intervals containing 68%, 95% and 99.9% probability for the ratio assuming the best fit parameters, respectively [26].

item	uncertainty on $T_{1/2}^{2\nu}$ (%)
non-identified background components	+5.3
energy spectra from $^{42}\text{K}$ , $^{40}\text{K}$ and $^{214}\text{Bi}$	$\pm 2.1$
shape of the $2\nu\beta\beta$ decay spectrum	$\pm 1$
subtotal fit model	+5.8 -2.3
precision of the Monte Carlo geometry model	$\pm 1$
accuracy of the Monte Carlo tracking	$\pm 2$
subtotal Monte Carlo	$\pm 2.2$
data acquisition and selection	$\pm 0.5$
Grand Total	+6.2 -3.3

**Table 2.** Summary table of the systematic uncertainties on  $T_{1/2}^{2\nu}$  which are taken into account for this work and which are not included in the fitting procedure.

As a cross-check, the same procedure is run for each detector separately. The resulting  $T_{1/2}^{2\nu}$  values are summarized in table 1; they are mutually consistent within their uncertainties ( $\chi^2/\nu = 3.02/5$ ).

#### 4.2. Systematic uncertainties

The items which are taken into account as possible systematic uncertainties of  $T_{1/2}^{2\nu}$  and which are not included in the fitting procedure are summarized in table 2. They can be divided into three main categories: (1) uncertainties related to the fit model (choice of the components, shape of input spectra); (2) uncertainties due to the Monte Carlo simulation regarding the precision of the geometry model and the accuracy of the tracking of particles; (3) uncertainties due to data acquisition and handling. The latter term turns out to be negligible with respect to the others. The most relevant items from table 2 are briefly discussed in the following.

Additional background components that are not accounted for in the fit model might be present in the GERDA spectrum (see ref. [10] for a list of the  $\gamma$ -ray lines detected in the GERDA spectrum and of the corresponding intensities). Due to the large signal-to-background ratio and the limited exposure these background components cannot be identified unambiguously. The uncertainty arising from such possible contributions is estimated to be +5.3%. Since any further background component would lead to a longer  $T_{1/2}^{2\nu}$ , this uncertainty is asymmetric. It is estimated by performing a fit with the contributions from  $^{60}\text{Co}$ ,  $^{228}\text{Ac}$ , and a flat background added to the model. These additional components are treated in the same way as the “standard” background components ( $^{42}\text{K}$ ,  $^{40}\text{K}$ , and  $^{214}\text{Bi}$ ). The spectra from  $^{60}\text{Co}$  and  $^{228}\text{Ac}$  are simulated by Monte Carlo assuming close sources and one additional parameter for each detector and each additional background contribution is included in the fit. Also for the flat background an individual contribution is considered for each detector. The flat component describes the contribution coming from  $^{208}\text{Tl}$  decays from the  $^{232}\text{Th}$  chain: given the small number of events expected in the analysis energy window, this contribution can be roughly approximated to be constant. To a first approximation, also other possible non-identified background components can be accounted by the constant contribution to the model.

The systematic uncertainty on  $T_{1/2}^{2\nu}$  due to the uncertainties in the spectra of the standard background components ( $^{42}\text{K}$ ,  $^{40}\text{K}$ , and  $^{214}\text{Bi}$ ) is estimated to be 2.1%. It is evaluated by repeating the analysis with different assumptions on the position and distribution of the sources and with artificial variations (e.g. via a scaling factor) of the ratio between the full-energy peaks and the Compton continua.

The primary spectrum of the  $2\nu\beta\beta$  decay which is fed into the Monte Carlo simulation is generated by the code DECAY0. DECAY0 implements the algorithm described in [3], which is based on [27, 28]. The  $2\nu\beta\beta$  decay distributions of [3] are in principle more precise than those based on the Primakoff-Rosen approximation [29]. They have been cross-checked against the high-statistics data of the NEMO experiment for several nuclei:  $^{82}\text{Se}$ ,  $^{96}\text{Zn}$  and  $^{150}\text{Nd}$  [30]. The  $2\nu\beta\beta$  spectrum derived by the Primakoff-Rosen approximation was used in earlier works with  $^{76}\text{Ge}$ , like [31]. When the present analysis is re-run by using the formula of [31], the  $T_{1/2}^{2\nu}$  result is stable within 1%.

The uncertainty related to the MAGE Monte Carlo simulation arises from two sources: (1) the implementation of the experimental geometry into the code (dimensions, displacements, materials); and (2) the interaction of radiation with matter (cross sections, final state distributions) which is performed by GEANT4. These items are evaluated to be 1% and 2%, respectively. The estimated contribution due to the particle tracking is based on the fact that electromagnetic physics processes provided by GEANT4 for  $\gamma$ -rays and  $e^\pm$  have been systematically validated at the few-percent level in the energy range which is relevant for  $\gamma$ -ray spectroscopy [32]. In this particular application the Monte Carlo uncertainty is mainly due to the propagation of the external  $\gamma$ -rays: the  $2\nu\beta\beta$ -decay electrons generated in the germanium detectors have a sub-cm range and they usually deposit their entire kinetic energy, apart from small losses due to the escape of Bremsstrahlung or fluorescence photons.

The combination in quadrature of the contributions reported in table 2 sums up to  ${}_{-3.3}^{+6.2}\%$ , corresponding to  ${}_{-0.06}^{+0.11} \cdot 10^{21}$  yr.

## 5. Results and conclusions

The half-life of the  $2\nu\beta\beta$  decay of  $^{76}\text{Ge}$  was derived from the first data from the GERDA experiment at the INFN Gran Sasso Laboratory. GERDA operates HPGe detectors enriched in  $^{76}\text{Ge}$  directly immersed in liquid argon. The analysis has been carried out on the data collected with six  $^{\text{enr}}\text{Ge}$  detectors (14.6 kg total weight) during 125.9 live days by fitting the energy spectra with a comprehensive model. The best estimate of the half-life of the  $2\nu\beta\beta$  decay is

$$T_{1/2}^{2\nu} = (1.84_{-0.08}^{+0.09}{}_{\text{fit}} \quad {}_{-0.06}^{+0.11}{}_{\text{sys}}) \cdot 10^{21} \text{ yr} = (1.84_{-0.10}^{+0.14}) \cdot 10^{21} \text{ yr}, \quad (2)$$

with the fit and systematic uncertainties combined in quadrature.

The half-life is longer than all previous measurements reported in the literature. A summary of the  $T_{1/2}^{2\nu}$  results of  $^{76}\text{Ge}$  from earlier experiments vs. publication year is displayed in figure 4. The figure includes nine measurements published between 1990 and 2005 and two weighted averages. A trend towards longer  $T_{1/2}^{2\nu}$  values reported by the most recent (and lowest background) experiments is clearly seen. The GERDA

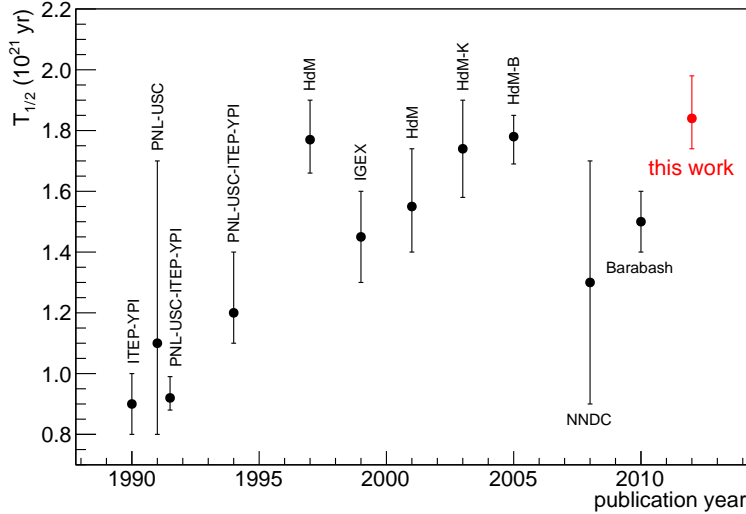


**Figure 4.** Experimental results for  $T_{1/2}^{2\nu}$  of  $^{76}\text{Ge}$  vs. publication year. The plot includes results from the experiments ITEP-YPI [33], PNL-USC ( $^{\text{nat}}\text{Ge}$ ) [34] PNL-USC-ITEP-YPI [35, 36], Heidelberg-Moscow (HdM) [11, 17] and IGEX [12, 16], as well as the re-analysis of the HdM data by Klapdor-Kleingrothaus *et al* [31] (HdM-K) and by Bakalyarov *et al* [37] (HdM-B). The NNDC-recommended value [38] and the global weighted average evaluated by Barabash [2] are also shown.

result is in better agreement with the two most recent results of [31, 37] that are based on the re-analysis of the HdM data\*. The fact that the half-lives derived in the more recent works – and particularly in this one – are systematically longer is probably related to the superior signal-to-background ratio, which lessens the relevance of the background modelling and subtraction. Thus the total GERDA uncertainty is comparable to what was achieved by HdM, in spite of the much smaller exposure.

The uncertainty of the GERDA result can be further reduced in the future by accumulating more exposure and by performing a new and more precise measurement of the active mass of the detectors. Large data sets will reduce also the uncertainty due to the fit model, as background components can be better characterized and constrained by the (non-)observation of  $\gamma$  lines.

Using phase space factors from the improved electron wave functions reported in [39], the experimental matrix element for the  $2\nu\beta\beta$  decay of  $^{76}\text{Ge}$  calculated with the half-life of this work is  $\text{NME}^{2\nu} = 0.133_{-0.005}^{+0.004} \text{ MeV}^{-1}$ .

The present value for  $\text{NME}^{2\nu}$  is 11 % smaller than that used in [5], which compares the matrix elements for  $2\nu\beta\beta$  and  $0\nu\beta\beta$  decays. Ref. [5] also shows a relation between the two matrix elements for QRPA calculations of  $^{76}\text{Ge}$ . According to this, the new value for  $\text{NME}^{2\nu}$  results in an increase of the predicted half-life for the  $0\nu\beta\beta$  by about

\* If  $T_{1/2}^{2\nu}$  were as short as  $1.5 \cdot 10^{21}$  yr reported in [2], the  $2\nu\beta\beta$  decay of  $^{76}\text{Ge}$  would account for nearly all counts detected in the range 600–1800 keV (expected: 8782.7, detected: 8976), thus leaving almost no space for any other background source in GERDA.

15%, which is well within the present uncertainty of the model calculation.

The nuclear matrix elements of the  $2\nu\beta\beta$  decay of  $^{76}\text{Ge}$  estimated from the charge exchange reactions (d, $^2\text{He}$ ) and ( $^3\text{He}$ ,t) are  $(0.159\pm 0.023)\text{ MeV}^{-1}$  [7] and  $(0.23\pm 0.07)\text{ MeV}^{-1}$  [8], respectively. They both seem to be higher than the value reported in this work, but consistent within the uncertainties.

## Acknowledgments

The GERDA experiment is supported financially by the German Federal Ministry for Education and Research (BMBF), the German Research Foundation (DFG) via the Excellence Cluster Universe, the Italian Istituto Nazionale di Fisica Nucleare (INFN), the Max Planck Society (MPG), the Polish National Science Centre (NCN), the Russian Foundation for Basic Research (RFBR), and the Swiss National Science Foundation (SNF). The institutions acknowledge also internal financial support.

The GERDA collaboration thanks the Directors and the staff of the Laboratori Nazionali del Gran Sasso for their continuous strong support of the experiment.

We would like to thank Prof. V.I. Tretyak for help and suggestions about the modelling of the energy spectrum of the  $2\nu\beta\beta$  decay.

## References

- [1] Avignone III F T, Elliott S R and Engel J 2008 *Rev. Mod. Phys.* **80** 481  
Gomez-Cadenas J J *et al* 2012 *Riv. Nuovo Cimento* **35** 29  
Vergados J D, Ejiri H and Simkovich F 2012 *Rep. Prog. Phys.* **75** 106301  
Bilenki S M and Giunti C 2012 *Mod. Phys. Lett. A* **27** 1230015  
Schwingenheuer B 2012 “Status and prospects of searches for neutrinoless double beta decay”, submitted to *Annalen der Physik*, preprint arXiv:1210.7432
- [2] Barabash A S 2010 *Phys. Rev. C* **81** 035501
- [3] Tretyak V I and Zdesenko Yu G 1995 *At. Data Nucl. Data Tables* **61** 43
- [4] Tretyak V I and Zdesenko Yu G 2002 *At. Data Nucl. Data Tables* **80** 83  
Ackerman N *et al* (EXO Collaboration) 2011 *Phys. Rev. Lett.* **107** 212501, arXiv:1108.4193v2  
Gando A *et al* (KamLAND-Zen Collaboration) 2012 *Phys. Rev. C* **85** 0455504, arXiv:1201.4664v2
- [5] Rodin V A, Fässler A, Šimkovic F and Vogel P 2006 *Nucl. Phys. A* **766** 107; erratum: **793** (2007) 213
- [6] Šimkovic F, Fässler A, Rodin V, Vogel P and Engel J 2008 *Phys. Rev. C* **77** 045503  
Šimkovic F, Hodak R, Fässler A and Vogel P 2011 *Phys. Rev. C* **83** 015502  
Caurier E, Nowacki F and Poves A 2012 *Phys. Lett. B* **711** 62  
Barea J and Iachello F 2009 *Phys. Rev. C* **79** 044301  
Suhonen J and Civitarese O 2012 *J. Phys. G: Nucl. Part. Phys.* **39** 085105  
Civitarese O and Suhonen J 2005 *Nucl. Phys. A* **761** 313
- [7] Greife E-W *et al* 2008 *Phys. Rev. C* **78** 044301
- [8] Ties J H *et al* 2012 *Phys. Rev. C* **86** 014304
- [9] GERDA Proposal to LNGS 2004 <http://www.mpi-hd.mpg.de/gerda/>
- [10] Ackermann K-H *et al* (GERDA Collaboration) 2012 “The GERDA experiment for the search of  $0\nu\beta\beta$  decay on  $^{76}\text{Ge}$ ”, submitted to *Eur. Phys. J. C*
- [11] Günther M *et al* 1997 *Phys. Rev. D* **55** 54
- [12] Morales A 1999 *Nucl. Phys. B. Proc. Suppl.* **77** 335
- [13] Barnabé Heider M 2009 “Performance and stability tests of bare high purity germanium detectors in liquid argon for the GERDA experiment”, Ph. D. thesis, U. Heidelberg, Germany; available at <http://www.ub.uni-heidelberg.de/archiv/9551>
- [14] Barnabé Heider M, Cattadori C, Chkvetseva O, di Vacri A, Gusev K, Schönert S and Shirchenko M 2008 IEEE Nuclear Science Symposium, Oct 19-25, N68-7
- [15] Riboldi S *et al* 2010 Proc. IEEE Nuclear Science Symposium and Int. Workshop on Room Temperature Semiconductor Detectors, Oct. 30 - Nov. 6, 1386
- [16] Morales J and Morales A 2003 *Nucl. Phys. B Proc. Suppl.* **114** 141

- [17] Klapdor-Kleingrothaus HV *et al* (Heidelberg-Moscow Collaboration) 2001 *Eur. Phys. J. A* **12** 147
- [18] Agostini M, Pandola L, Zavarise P and Volynets O 2011 *JINST* **6** P08013
- [19] Agostini M, Pandola L and Zavarise P 2012 *J. Phys. (Conf. Ser.)* **368** 012047  
Agostini M 2012 Ph.D. thesis, Tech. U. Munich, Germany; in preparation
- [20] Caldwell A and Kröninger K 2006 *Phys. Rev. D* **74** 092003
- [21] Boswell M *et al* 2011 *IEEE Trans. Nucl. Sci.* **58** 1212
- [22] Agostinelli S *et al* (Geant4 Collaboration) 2003 *Nucl. Instrum. Methods A* **506** 250  
Allison J *et al* (Geant4 Collaboration) 2006 *IEEE Trans. Nucl. Sci.* **53** 270
- [23] Ponkratenko O A, Tretyak V I and Zdesenko Yu G 2000 *Phys. Atom. Nuclei* **63** 1282
- [24] Caldwell A, Kollar D and Kröninger K 2009 *Comput. Phys. Comm.* **180** 2197
- [25] Beaujean F, Caldwell A, Kollar D and Kröninger K 2011 *Phys. Rev. D* **83** 012004
- [26] Aggarwal R and Caldwell A 2012 *Eur. Phys. J. Plus* **127** 24
- [27] Doi M, Kotami T, Nishira H, Okuda K and Takasugi E 1981 *Progr. Theor. Phys.* **66** 1739  
Mohapatra R N and Takasugi E 1988 *Phys. Lett. B* **211** 192  
Burgess C P and Cline J M 1993 *Phys. Lett. B* **298** 141  
Carone C D 1993 *Phys. Lett. B* **309** 85
- [28] Blatt J M and Weisskopf V F 1963 *Theoretical Nuclear physics 7<sup>th</sup>* Ed. (New York: John Wiley)
- [29] Primakoff H and Rosen S P 1959 *Rep. Prog. Phys.* **22** 121
- [30] Arnold R *et al* (NEMO Collaboration) 1998 *Nucl. Phys. A* **636** 209  
Arnold R *et al* (NEMO Collaboration) 1999 *Nucl. Phys. A* **658** 299  
Arnold R *et al* (NEMO Collaboration) 2000 *Nucl. Phys. A* **678** 341  
Arnold R *et al* (NEMO Collaboration) 2006 *Nucl. Phys. A* **765** 483  
Argyriades J *et al* (NEMO Collaboration) 2009 *Phys. Rev. C* **80** 032501
- [31] Dörr C and Klapdor-Kleingrothaus H V 2003 *Nucl. Instrum. Methods A* **513** 596
- [32] Amako K *et al* 2005 *IEEE Trans. Nucl. Sci.* **52** 910  
Poon E and Verhaegen F 2005 *Med. Phys.* **32** 1696  
Cirrone G A P, Cuttone G, Di Rosa F, Pandola L, Romano F and Zhang Q 2010 *Nucl. Instrum. Methods A* **618** 315
- [33] Vasenko A A *et al* 1990 *Mod. Phys. Lett. A* **5** 1299
- [34] Miley H S *et al* 1990 *Phys. Rev. Lett.* **65** 3092
- [35] Avignone F T *et al* 1991 *Phys. Lett. B* **256** 559
- [36] Avignone F T *et al* 1994 *Prog. Part. Nucl. Phys.* **32** 223
- [37] Bakalyarov A M, Balysh A Y, Belyaev S T, Lebedev V I and Zhukov S V 2005 *Phys. Part. Nucl. Lett.* **2** 77; *Pisma Fiz. Elem. Chast. Atom. Yadra* **2** 21, preprint arXiv:hep-ex/0309016
- [38] Pritychenko B 2008 *Nuclear Structure 2008* June 3-6 2008, East Lansing, MI
- [39] Kotila J and Iachello F 2012 *Phys. Rev. C* **85** 034316